Longitudinal and transverse Hall resistivities in $NaFe_{1-x}Co_xAs$ single crystals with $x$ = 0.022 and 0.0205: weak pinning and anomalous electrical transport properties



2013 J. Phys.: Condens. Matter 25 395702

(http://iopscience.iop.org/0953-8984/25/39/395702)

IOP PUBLISHING JOURNAL OF PHYSICS: CONDENSED MATTER
J. Phys.: Condens. Matter **25** (2013) 395702 (8pp) doi:10.1088/0953-8984/25/39/395702

# Longitudinal and transverse Hall resistivities in $NaFe_{1-x}Co_xAs$ single crystals with $x = 0.022$ and 0.0205: weak pinning and anomalous electrical transport properties

**L M Wang[1], Chih-Yi Wang[1], Un-Cheong Sou[1], H C Yang[2], L J Chang[3], Caleb Redding[4], Yu Song[5], Pengcheng Dai[5] and Chenglin Zhang[4,5]**

[1] Graduate Institute of Applied Physics/Department of Physics, National Taiwan University, Taipei 106, Taiwan
[2] Department of Electro-optical Engineering, Kun Shan University, Tainan County 710, Taiwan
[3] Department of Physics, National Cheng Kung University, Tainan 70101, Taiwan
[4] Department of Physics and Astronomy, The University of Tennessee, Knoxville, TN 37996-1200, USA
[5] Department of Physics and Astronomy, Rice University, Houston, TX 77005, USA

E-mail: liminwang@ntu.edu.tw

Received 23 July 2013, in final form 14 August 2013
Published 4 September 2013
Online at stacks.iop.org/JPhysCM/25/395702

**Abstract**
The in-plane longitudinal and Hall resistivities, $\rho_{xx}$ and $\rho_{xy}$, of superconducting $NaFe_{1-x}Co_xAs$ (NFCA) single crystals with $x = 0.022$ and 0.0205 in the mixed state and the normal state were measured to study the electrical transport properties in nearly optimum-doping iron-based superconductors. The resistivities under magnetic fields show thermally activated behavior and a power law magnetic field dependence of activation energy has been obtained. Due to the weak flux pinning, there is no sign reversal of Hall resistivities observed for NFCA with either $x = 0.022$ or 0.0205. The correlation between longitudinal and Hall resistivities shows that the scaling behavior of $|\rho_{xy}| \propto (\rho_{xx})^{\beta}$ with the exponent $\beta \approx 2.0$ is in agreement with theoretical predictions for weak-pinning superconductors. Anisotropic upper critical fields and coherence lengths with an anisotropy ratio of $\gamma \approx 1.63$ have been deduced. Furthermore, the normal-state transport properties show that the anomalies of the linear-$T$ resistivity, the $T^2$-dependent cotangent of the Hall angle, the linear-$T$-like Hall number, and the magnetoresistance, which can be scaled by the modified Kohler rule, are analogous to those observed on optimally doped high-$T_c$ superconducting cuprates and other pnictides. The longitudinal resistivity can be understood within a widely accepted scenario of the spin density-wave quantum critical point, while the transverse resistivity requires some further explanation. It is suggested that all the transport anomalies should be simultaneously taken into account when developing theory.

(Some figures may appear in colour only in the online journal)

## 1. Introduction

The superconductivity discovered in iron-based pnictides has attracted considerable interest in recent times [1–3]. Being similar to high-$T_c$ superconducting (HTS) cuprates, the new iron-based superconductors have rich transport properties both in the mixed state and the normal state. The microscopic origin of anomalous non-Fermi-liquid $T$-linear

 

resistivity, $T$-dependent Hall coefficient $R_H$, and the sign change of $R_H$ observed both in the normal state and the mixed state remains a subject of debate. To date, mixed-state transport-property studies have shown low anisotropy, weak thermal fluctuation, and relatively weak vortex pinning associated with a small thermally activated energy in these iron-based superconductors [4–8]. Measurements of the longitudinal and Hall resistivities have been extremely useful in revealing mixed-state vortex dynamics and even the relation between antimagnetism and superconductivity in these novel materials [9]. Among the electrical transport studies on iron-based pnictides, however, few studies [10–14] have explored the transport properties of the doped NaFeAs system (the so-called Na111 system) because of the difficulty in growing high-quality single crystals and the instability due to high interaction with the environment [13]. It has been reported that doping with Co in NaFeAs, $NaFe_{1-x}Co_xAs$ (NFCA), reveals a phase diagram which is matched well to the phase diagram of $Ba(Fe_{1-x}Co_x)As_2$ [10, 11], and is expected to be a simplified version of the structures of ReFeAsO (the so-called 1111 system, Re = rare earth) and doped $AeFe_2As_2$ (the so-called 122 system, Ae = Ca, Sr, Ba and Eu) pnictides [12]. Thus, examining the nature of electrical transport in NFCA can improve the general understanding of the superconductivity and their normal-state properties. In this work, we study the mixed-state and normal-state transport properties of NFCA single crystals with $x = 0.022$ and 0.0205. In this paper we show in full detail the electrical transport properties of NFCA, including the mixed-state Hall effect, the scaling behavior, the normal-state Hall angle, and the magnetoresistance in the normal state, which still need to be examined. All the results are discussed within existing theorems and compared with previous findings related to high-$T_c$ superconducting cuprates and other pnictides to reveal the fundamental superconducting properties of NFCA.

## 2. Experimental details

Single crystals of NFCA with $x = 0.022$ and 0.0205 were grown by sealing a mixture of Na, Fe, and Co together in Ta tubes and heating at 950 °C, followed by 5 °C $h^{-1}$ cooling to 900 °C. The crystals were well-formed slabs with $c$-axis orientation perpendicular to the plane of the crystal slabs, as described previously [13]. The real composition of crystals was identified by an inductively coupled plasma spectrometer and showed a tiny evaporation of Na during the sample growth. For in-plane transport measurements, the samples were cleaved from the inner part of the crystals and cut into dimensions of around $4 \times 1.5 \times 0.05$ $mm^3$. Five leads were glued with silver paste and a Hall-measurement geometry was constructed to allow simultaneous measurements of both longitudinal ($\rho_{xx}$) and transverse (Hall) resistivities ($\rho_{xy}$) using the standard dc four-probe technique. The contact size was miniaturized to be as small as possible (<0.5 mm) to avoid large inaccuracy in resistivity calculation. Hall voltages were taken in opposing fields parallel to the $c$-axis up to 6 T and at an in-plane current density of ~30 A $cm^{-2}$. All the sample preparations were done quickly in dry inert helium gas to prevent interaction with the environment.

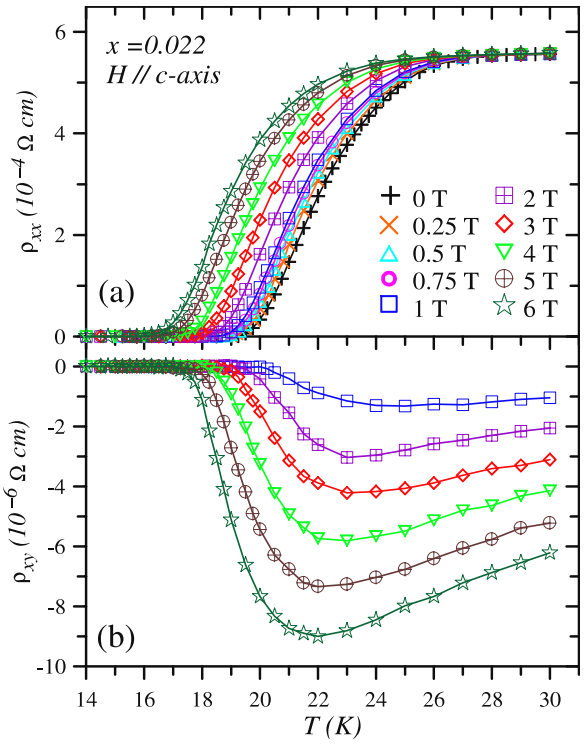


**Figure 1.** Temperature dependence of (a) $\rho_{xx}$ and (b) $\rho_{xy}$ with magnetic fields parallel to the crystal $c$ axis for NFCA with $x = 0.022$.

## 3. Results and discussion

Longitudinal and Hall resistivities, $\rho_{xx}$ and $\rho_{xy}$, in the presence of magnetic fields for NFCA crystals in the mixed state were systematically investigated. Figures 1(a) and (b) respectively show the resistivities, $\rho_{xx}$ and $\rho_{xy}$, as a function of temperature in magnetic fields for the NFCA crystal with $x = 0.022$. Figures 2(a) and (b) respectively show $\rho_{xx}$ and $\rho_{xy}$ as a function of temperature in magnetic fields for the NFCA crystal with $x = 0.0205$. The negative Hall resistivity $\rho_{xy}$ reveals an electron-dominating transport, and gradually becomes zero with decrease in temperature, where the resistivity $\rho_{xy}$ does not go into a sign reversal in the mixed state. The superconducting critical temperatures $T_c$, determined by choosing the point of the 50% zero-field resistive transition, are 22.1 and 20.9 K for NFCA samples with $x = 0.022$ and 0.0205, respectively. The data of $T_c$ and longitudinal resistivity are similar to those previously reported [10–14], while the data of mixed-state Hall (transverse) resistivity for NFCA, to the best of our knowledge, are reported for the first time.

In figures 1(a) and 2(a), the longitudinal resistivity shows typical broadening behavior due to thermally activated flux motion, and can be described by [15, 16]

$$\rho_{xx}(T, H) = \rho_0 \exp(-U/k_B T). \quad (1)$$

Here $U$ is the activation energy, which is normally both field- and temperature-dependent, which is an indication of the magnitude of effective pinning energy. Figure 3(a) shows the field-dependent activation energy extracted from (1) via

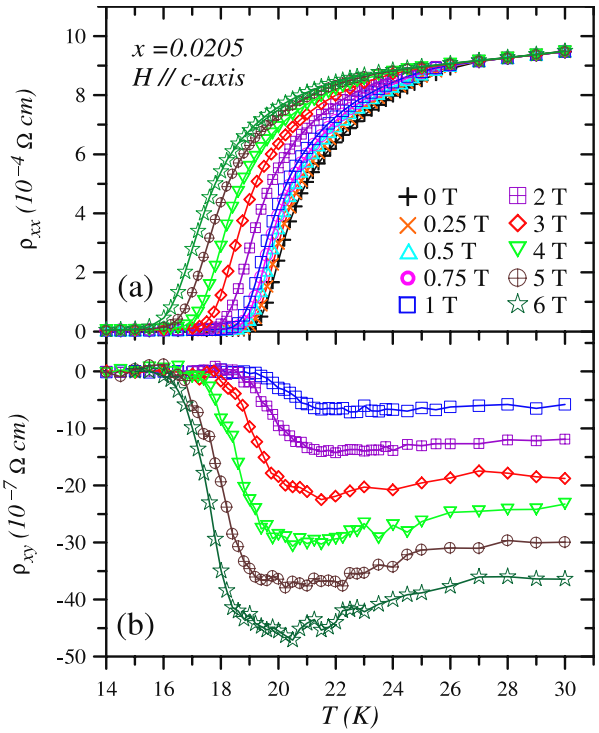


**Figure 2.** Temperature dependence of (a) $\rho_{xx}$ and (b) $\rho_{xy}$ with magnetic fields parallel to the crystal $c$ axis for NFCA with $x = 0.0205$.

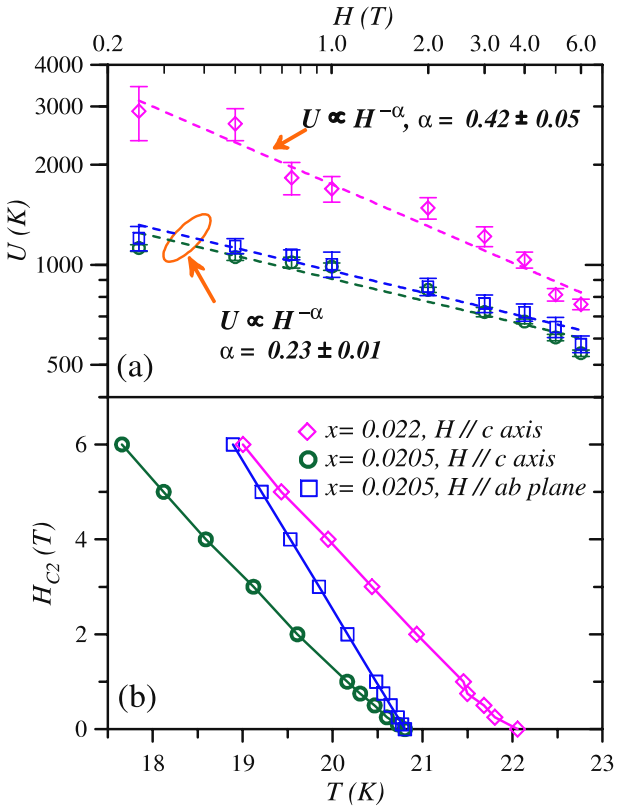


**Figure 3.** (a) Field-dependent activation energy for NFCA crystals with $x = 0.022$ and 0.0205. The dashed lines indicate the fitting of $U \propto H^{-\alpha}$. (b) Upper critical fields $H_{c2,c}$ and $H_{c2,ab}$ as a function of temperature for NFCA with $x = 0.022$ and 0.0205.

the Arrhenius plots for NFCA with $x = 0.022$ and 0.205 crystals. As seen, the activation energies for NFCA with $x = 0.022$ are rather larger than those for NFCA with $x = 0.0205$. Meanwhile, in NFCA with $x = 0.0205$, the values of $U$ for fields applied parallel to the *ab* plane are slightly larger than those for fields applied parallel to the $c$ axis. The values of $U$ for NFCA, ranging from 600 K at magnetic field $H = 6$ T to 3000 K ($H = 0.25$ T), are approximately one order of magnitude smaller than those of several $10^4$ K for $YBa_2Cu_3O_y$ (YBCO) [17], and several times smaller than those of 3000–7000 K for $Ba(Fe_{1-x}Co_x)As_2$ [18]. The obtained $U$ values for NFCA are slightly larger than those of 100–200 K for Fe(Te, S) single crystals [7]. This indicates a relatively weak vortex pinning in NFCA and Fe(Te, S) systems (the so-called 111 and 11 systems, respectively). The critical current density $J_c$ for our samples can be derived (according to the Bean model) from the magnetization hysteresis-loop measurement performed by another research group [10]. Indeed the $J_c$ of around $10^4$ A cm$^{-2}$ at 5 K is lower than that of $>10^5$ A cm$^{-2}$ for $Ba(Fe_{1-x}Co_x)As_2$ [18]. This weak vortex pinning may lead to the result that no sign reversal of $\rho_{xy}$ can be observed both in NFCA with $x = 0.022$ and 0.0205 crystals, as seen in figures 1(b) and 2(b), respectively. It is known that the sign reversal of $\rho_{xy}$ in the mixed state (the so-called anomalous mixed-state Hall effect) of type-II superconductors has been one of the most interesting subjects in the past two decades. Many theoretical or experimental studies have pointed out that a strong vortex pinning can result in an anomalous Hall effect [19–21]. Apparently the disappearance of anomalous Hall effect observed in the weak-pinning NFCA is consistent with these arguments. It is noted that the $Ba(Fe_{1-x}Co_x)_2As_2$ film with high-density pinning centers does not exhibit any sign reversal of Hall resistivity as recently reported by Sato *et al* [22]. Their observation is similar to that in an experiment of Budhani *et al* [23] where a diminishing sign anomaly of the mixed-state Hall resistivity in $Tl_2Ba_2Ca_2Cu_3O_{10}$ films with increasing columnar defects was reported. The phenomenon of diminishing sign anomaly with increasing pinning centers has been commented on by Wang *et al* [19] who claimed that the effective pinning could be decreased due to a lower condensation energy density even though the number of pinnings is increased, and then the sign anomaly diminishes. In fact, from the $\rho_{xx}$ data of Sato *et al* we can derive the activation energy and have $U(1\text{ T})$ of around 2300 K for their $Ba(Fe_{1-x}Co_x)_2As_2$ film, which is much lower than those obtained in the $Ba(Fe_{1-x}Co_x)_2As_2$ single crystals [18]. Thus it is not surprising that there is no sign reversal of Hall resistivity observed in the $Ba(Fe_{1-x}Co_x)_2As_2$ film.

It is also found that $U$ at fields $\leq 5$ T can be fitted with an approximate field dependence of $U \propto H^{-\alpha}$ with $\alpha = 0.42$ and 0.23 for NFCA with $x = 0.022$ and 0.0205 crystals, respectively, as shown in figure 3(a), similar to those observed in high-$T_c$ superconducting cuprates [17, 24, 25] or other pnictides [7, 8, 18]. Some experimental data show that $U$ is proportional to $H^{-\alpha}$ with $\alpha = 0.76$–$0.88$, $0.33$–$0.50$, and $0.44$–$0.79$ for YBCO films [24], $Bi_2Sr_2CaCu_2O_8$ [25],

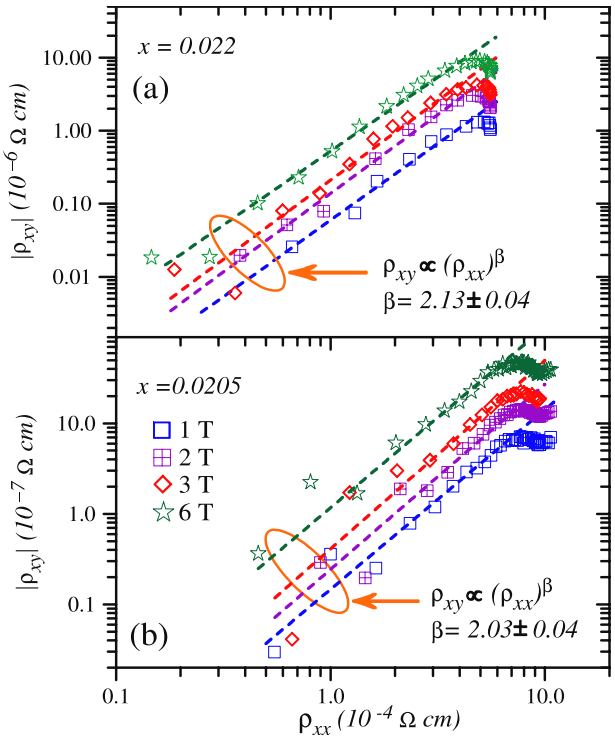


**Figure 4.** Plots of $\log|\rho_{xy}|$ versus $\log\rho_{xx}$ taken at fixed magnetic fields for NFCA with (a) $x = 0.022$ and (b) $x = 0.0205$. The dashed lines indicate the fitting of $\rho_{xy} \propto (\rho_{xx})^{\beta}$.

and YBCO/$PrBa_2Cu_3O_y$ superlattices [17], respectively. The power law dependence of $U$ with $\alpha = 0.5$ has been proposed for YBCO crystals within the plastic vortex creep model [26]. Obviously, the activation energy does not scale with the predicted $H^{-1}$ dependence [27] or the $H^{-0.5}$ dependence. Comparable values of $\alpha$ ranging from 0.21 to 0.38 have recently been obtained in Fe(Te, S) [7], FeSe [8], and $Ba(Fe_{1-x}Co_x)As_2$ single crystals [18], while a much slower field dependence of $U$ with $U \propto H^{-0.13}$ has been reported in $Ba_{0.72}K_{0.28}Fe_2As_2$ single crystals [28]. The deviation of $\alpha$ from the value of 0.5 for these single-crystal pnictides could result from the crossover in flux dynamics from elastic to plastic creep as seen in YBCO crystals [26], or could be attributed to the flux dynamics dominated by single-vortex pinning in the low-field region [29]. Figure 3(b) shows the upper critical field $H_{c2,c}$ as a function of temperature for NFCA with $x = 0.022$ and 0.0205 crystals in the magnetic field parallel to the crystal $c$ axis. Moreover, the in-plane upper critical fields $H_{c2,ab}(T)$ for NFCA with $x = 0.0205$ crystals are also shown in figure 3(b). Here the upper critical field corresponding to the temperature is derived from the 50% resistive transition. The $H_{c2,c}(T)$ and $H_{c2,ab}(T)$ show linear behavior for the temperatures near $T_c$. Furthermore, the value of the zero-temperature upper critical field, $H_{c2}(0)$, can be derived using the formula $H_{c2}(0) = 0.693T_c\,|dH_{c2}(T)/dT|_{T_c}$ [30] where the slope $|dH_{c2}(T)/dT|$ can be obtained from the linear-fitting in figure 3(b). The values of $H_{c2,c}(0)$ are 31.2 ± 0.3 and 27.9 ± 0.4 T respectively for NFCA with $x = 0.022$ and 0.0205 crystals, while $H_{c2,ab}(0) = 45.4 \pm 0.1$ T is achieved for NFCA with $x =$ 0.0205 crystal. Having the values of $H_{c2,c}(0)$ and $H_{c2,ab}(0)$, we can obtain the coherence lengths, $\xi_{ab}(0)$ and $\xi_c(0)$, and even derive the anisotropy ratio, $\gamma = \xi_{ab}/\xi_c$. It is known that the coherence lengths, $\xi_{ab}$ and $\xi_c$, in the anisotropic Ginzburg–Landau theory are related to the upper critical fields, $H_{c2,c}$ and $H_{c2,ab}$, by the formulas

$$\xi_{ab} = (\Phi_0/2\pi H_{c2,c})^{0.5} \quad (2)$$

$$\xi_c = (\Phi_0/2\pi H_{c2,ab})/\xi_{ab}, \quad (3)$$

where $\Phi_0 = hc/2e$ is the flux quantum. The values of $\xi_{ab}(0)$ for NFCA with $x = 0.022$ and 0.0205 are 32.5 ± 0.2 and 34.4 ± 0.3 Å, respectively, while $\xi_c(0) = 21.1 \pm 0.3$ Å is obtained for the NFCA with $x = 0.0205$. Using (2) and (3), we also have the anisotropy ratio, $\gamma = \xi_{ab}/\xi_c = H_{c2,ab}/H_{c2,c} = 1.63 \pm 0.04$, for the NFCA sample with $x = 0.0205$. The obtained coherence lengths for NFCA single crystals are larger than the reported values of $\xi_{ab}(0) \approx 16$–24 Å and $\xi_c(0) \approx 3$–7 Å for YBCO [31]. Meanwhile, typical values of anisotropy ratio for HTS cuprates are 5–8, 55–150, and 70–350 for YBCO [32, 33], $Bi_2Sr_2CaCu_2O_y$ [34, 35] and $Tl_2Ba_2CaCu_2O_y$ [36, 37] respectively. Obviously, the anisotropy ratio $\gamma$ for NFCA is much smaller than those for HTS cuprates. Here the obtained value of $\gamma$ for NFCA with $x = 0.0205$ is close to that of 2.25 for NFCA with $x = 0.025$ [13], and 2.0 for $(Ca_{0.33}Na_{0.66})Fe_2As_2$ [4] or $Sr_{0.6}K_{0.4}Fe_2As_2$ [38]. The values of anisotropy ratio $\gamma$ for other iron-based pnictides have been reported to be 2.5–3 for hole- and electron-doped $BaFe_2As_2$ [5], and 4–5 for F-doped NdFeAsO [39, 40], which are slightly higher than the obtained value for NFCA.

An interesting feature in the mixed-state transport properties is the scaling behavior, $\rho_{xy} \propto (\rho_{xx})^{\beta}$, which has attracted much attention. Figures 4(a) and (b) demonstrate the plots of $\log|\rho_{xy}|$ versus $\log\rho_{xx}$ at fixed magnetic fields for NFCA with $x = 0.022$ and 0.0205, respectively. The data display the power law relationship encompassing a variation in $\rho_{xy}$ of around two orders of magnitude, following the power law relationship with $\beta = 2.13 \pm 0.04$ and $2.03 \pm 0.04$ for NFCA with $x = 0.022$ and 0.0205 crystals, respectively. Many efforts, both theoretical and experimental studies, have been put forward to explore scaling behavior. In experiments, this scaling law was first observed by Luo *et al* [41] for YBCO films with $\beta = 1.7 \pm 0.2$ and by Samoilov *et al* [42] for $Bi_2Sr_2CaCu_2O_y$ single crystals with $\beta = 2.0 \pm 0.1$. The scaling behavior was also found in $MgB_2$ films [43], the $Ba(Fe_{0.9}Co_{0.1})As_2$ crystal [18], and the Fe(Te, S) crystal [7] with $\beta = 2.0 \pm 0.1$, $2.0 \pm 0.2$, and 0.9–1.0, respectively. Since then, various $\beta$ values have been reported; indeed, Hall scaling behavior is a complicated phenomenon, and a number of theories have been proposed to account for it. Dorsey and Fisher [44] demonstrated that the scaling behavior is a consequence of the vortex motion near the glass transition and obtained an appropriate valve of $\beta = 1.7$. Vinokur *et al* [45] considered the effects of flux pinning on Hall resistivities in the thermally assisted flux-flow region and showed that $\beta = 2.0$. Wang *et al* [19] also developed a unified theory for the anomalous Hall effect including both the flux pinning effect and thermal fluctuations. They demonstrated that the scaling

exponent $\beta$ changes from 2 to 1.5 with increased pinning. Here the exponent $\beta \approx 2.0$ for NFCA single crystals is in agreement with the predictions in theories or experiments on superconductors with weaker pinning, and is consistent with the relatively low activation energy as previously observed in mixed-state longitudinal resistivities.

In addition to the mixed-state properties, for the general understanding superconductivity in iron pnictide superconductors, it is of crucial importance to clarify the normal-state charge transport. In this family of Na111, a linear-$T$ resistivity at optimum doping has been observed, giving the scenario of spin density-wave (SDW) quantum critical point (QCP) to describe the normal-state transport properties [10, 14]. It has even been proposed that the SDW QCP is a central organizing principle of organic, iron pnictide, heavy-fermion, and HTS cuprates [9, 46]. Under QCP (i.e. optimum doping), the strongest magnetic spin fluctuation suppresses the SDW order, accompanying the appearance of the highest $T_c$, and results in non-Fermi-liquid-like scattering (linear-$T$ resistivity) associated with Fermi-surface reconstruction. For nearly optimum-doped NFCA with $x = 0.022$ and 0.0205, the temperature dependences of normal-state longitudinal resistivity, the Hall coefficient, and carrier concentration are shown in figures 5(a), (b), and (c), respectively. A linear-$T$ resistivity for temperatures above $T_c$ can be observed both on NFCA with $x = 0.022$ and 0.0205 as seen in figure 5(a). It has been suggested that the linear temperature dependence of resistivity may be the usual behavior resulting from electron–phonon interaction for $T > \theta_D/4$ [47], where $\theta_D$ is the Debye temperature. $\theta_D$ can be determined by the Debye $T^3$ approximation of low-temperature lattice specific heat $C_{\text{lattice}}(T)$ measurement. Taking account of $C_{\text{lattice}}(T) \approx \beta_c T^3$ associated with $\beta_c = 0.23$ mJ mol$^{-1}$ K$^{-4}$ reported for NFCA with $x = 0.028$ [12], we obtain $\theta_D \approx 200$ K for NFCA. Thus the origin of linear-$T$ resistivity for temperatures below $\theta_D/4 \approx 50$ K due to electron–phonon interaction can be excluded. Therefore the resistivity from 27 K up to 50 K is fitted by a function of the form $\rho_{xx} = \rho_0 + AT$ as shown in figure 5(a). Recently, the strength of the linear term, measured by the $A$ coefficient, has been found to scale with the superconducting transition temperature $T_c$ for Bechgaard salts and $Ba(Fe_{1-x}Co_x)_2As_2$ [48], in which the values of coefficient $A$ are 0.35 and 0.5 $\mu\Omega$ cm K$^{-1}$ for the highest-$T_c$ Bechgaard salts and $Ba(Fe_{1-x}Co_x)_2As_2$, respectively. Here the obtained coefficient $A$ is around 2.2 (11.0) $\mu\Omega$ cm K$^{-1}$ for nearly optimum-doped NFCA with $x = 0.022$ (0.0205), which is a little larger than those for the Bechgaard salts and $Ba(Fe_{1-x}Co_x)_2As_2$, or the value of 0.6 $\mu\Omega$ cm K$^{-1}$ for optimum-doped $La_{2-x}Ce_xCuO_4$ [46]. This common feature observed in different families of superconductors strongly suggests that the linear-$T$ resistivity of NFCA is also caused by spin fluctuation. The linear-$T$ resistivity and the existence of a quantum critical point at the optimal doping for $Na_{1-\delta}FeAs$ or NFCA have also been proposed [10, 14].

Furthermore, in addition to the behavior of linear-$T$ resistivity, the strong temperature dependence of the Hall coefficient $R_H$ of the HTS cuprates or pnictides has been

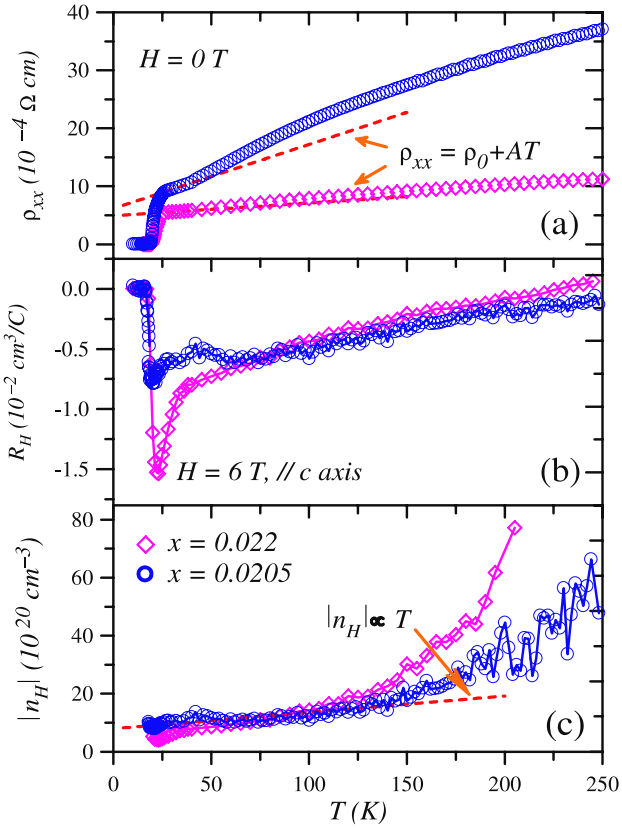


**Figure 5.** (a) Temperature-dependent in-plane resistivity in samples of NFCA with $x = 0.022$ and 0.0205 in $H = 0$ T. The dashed lines denote the fit of the form $\rho_{xx} = \rho_0 + AT$ at temperatures of 27–50 K. (b) Temperature dependence of Hall coefficient $R_H$ for NFCA with $x = 0.022$ and 0.0205 in $H = 6$ T. (c) Temperature dependence of Hall number $|n_H| = 1/(e|R_H|)$ for NFCA with $x = 0.022$ and 0.0205.

considered to be one of the most peculiar properties of the unusual normal state [9, 49, 50]. Indeed a marked temperature dependence of $R_H$ for NFCA with $x = 0.022$ and 0.0205 can be observed as shown in figure 5(b). The negative sign of $R_H$ indicates that electrons are responsible for the dominant contribution to the electric transport, which leads to expectation that the variation of Hall number $n_H = 1/(eR_H)$ is governed by the temperature-dependent concentration of electrons. A linear-$T$-like $|n_H(T)|$ for NFCA with $x = 0.022$ and 0.0205 can be observed at temperatures below 150 K as shown in figure 5(c). In figure 5(a) we also note that there is a little difference between the two $\rho_{xx}(T)$ plots but the basic features are very similar, as well as the characteristic temperatures for the two samples with near compositions. It has been proposed that due to softness of the pnictide materials, the cracks induced during their cutting and shaping into transport samples will affect the effective geometric factors of the sample, as discussed fully by Tanatar *et al* [51]. Thus it can be assumed that cracks or exfoliations internal to the sample are responsible for the resistivity difference. However this problem does not influence any behavior discussed here.

So far, it has been found that these normal-state properties of NFCA, including the linear-$T$ resistivity,

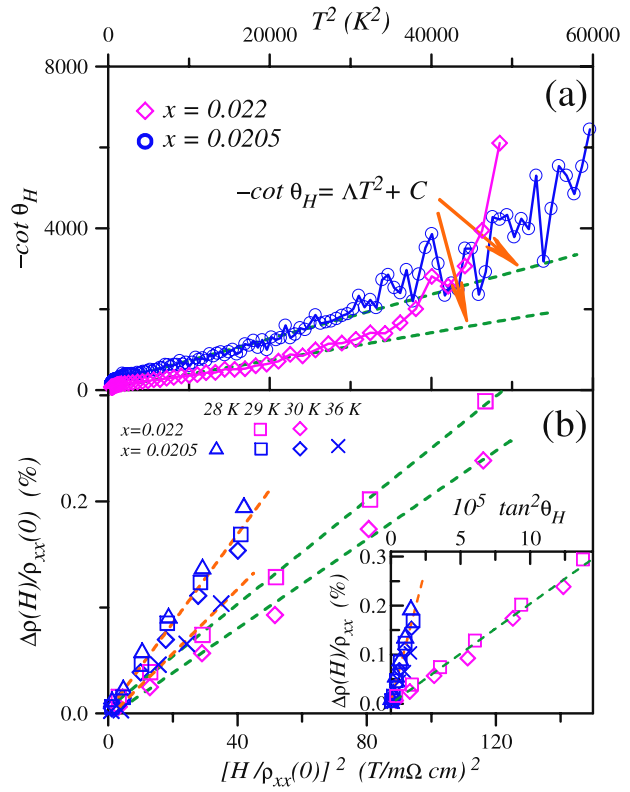


**Figure 6.** (a) Temperature dependence of the Hall angle shown as $\cot\theta_{\rm H}$ versus $T^2$ for NFCA with $x = 0.022$ and 0.0205 measured in $H = 6$ T. The dashed lines indicate the fitting of $\cot\theta_{\rm H} = \Lambda T^2 + C$. (b) Magnetoresistance $\Delta\rho(H)/\rho_{xx}(0)$ plotted as a function of $[H/\rho_{xx}(0)]^2$ for NFCA with $x = 0.022$ and 0.0205. The inset shows $\Delta\rho(H)/\rho_{xx}(0)$ plotted as a function of $\tan^2\theta_{\rm H}$. The dashed lines are guides to the eye.

strongly $T$-dependent $R_{\rm H}$, and linear-$T$-like $|n_{\rm H}(T)|$, are similar to those observed in HTS cuprates [9, 46, 49] or other pnictides [48, 50], and can be regarded as an anomalous feature in comparison with conventional metals. In fact, $R_{\rm H}$ itself is complex and many different explanations have been proposed for the anomalous normal-state Hall effect observed in HTS cuprates. A widely known approach proposed by Anderson [52] argues that the system has non-Fermi-liquid (Luttinger liquid) properties, and the temperature dependence of $R_{\rm H}(T)$ could be better understood in terms of two apparently decoupled scattering rates with the spin–charge separation scenario. Anderson revealed the clue to perceiving the normal-state Hall anomaly by distinguishing between the transport scattering rate, $1/\tau_{\rm tr}$ (varies linearly with temperature), and Hall relaxation rate, $1/\tau_{\rm H}$ (a $T^2$ process), for the carrier motion. The theory particularly predicts the $T^2$ behavior of the cotangent of the Hall angle, $\cot\theta_{\rm H} \equiv \rho_{xx}/\rho_{xy}$, and has been applied to the dc and ac Hall effects in high-$T_{\rm c}$ superconductors [53–55].

In figure 6(a) we plot $\cot\theta_{\rm H}$ versus $T^2$ for NFCA with $x = 0.022$ and 0.0205 measured in the field of 6 T. As can be seen, the data almost fall on a straight line in the temperature range below ∼170 K, and can be fitted to the equation of $-\cot\theta_{\rm H} = \Lambda T^2 + C$ with the parameters $\Lambda$ and $C$ of 34.1 (54.6) mK$^{-2}$ and 53.8 (178.7) for NFCA with $x = 0.022$ (0.0205). The values of $\Lambda$ and $C$ are slightly larger than those observed in HTS cuprates [53] and $Ba(Fe_{1-x}Co_x)_2As$ single crystals [18]. Another theoretical approach, the so-called nearly antiferromagnetic Fermi liquid (NAFL) theory [56, 57], argues that the system is still a Fermi liquid, relying on an anisotropic reconstruction of the Fermi surface in the presence of magnetic spin fluctuation. In the NAFL model the transport properties are governed by only one scattering rate, $1/\tau$, which is strongly dependent on the position on the Fermi surface of the quasiparticles in the well-established Fermi liquid state. In addition, a transport theory involving resistivity and the Hall coefficient on the basis of the microscopic Fermi liquid theory has been developed by considering the current vertex correction (CVC). This theory also supports the idea that HTS cuprates are still Fermi liquids with strong antiferromagnetic fluctuations [49]. The Fermi liquid descriptions seem to account for a wide doping range in HTS cuprates [49, 57]. In addition to these mentioned theoretical schemes, many approaches, such as the anisotropic marginal Fermi liquid (MFL) model [58, 59], the two-band scenario associated with the Coulomb interaction in excitons [60], and the model of coexisting holes and electrons with different effective mass [61], have been proposed for the anomalous transport phenomena in HTS cuprates as described in some review articles [9, 49]. All these developed theories try to succeed in reproducing various non-Fermi-liquid-like behaviors in the normal state of HTS cuprates. Moreover, another pronounced non-Fermi-liquid characteristic is the modified Kohler scaling which relates the magnetoresistance with the resistivity and Hall angle [9, 62]. In conventional metals, the magnetoresistance $\Delta\rho(H)/\rho_{xx}(0) \equiv [\rho_{xx}(H) - \rho_{xx}(0)]/\rho_{xx}(0)$ due to an orbital motion of carriers can be scaled as a function of the term $H/\rho_{xx}(0)$, being regarded as following Kohler's scaling rule. However, it has been demonstrated that this scaling clearly breaks down in cases of optimum-doped YBCO, $La_{2-x}Sr_xCuO_4$, and $BaFe_2(As_{1-x}P_x)_2$ [62, 63]. It has been shown that the $\Delta\rho/\rho_{xx}$ can be fitted to be proportional to the term $[H/\rho_{xx}(0)]^2$ with a slope that is temperature dependent, which is a violation of Kohler's scaling, and may be scaled by the square of the Hall angle as $\Delta\rho(H)/\rho_{xx}(0) \propto \tan^2\theta_{\rm H}$ (modified Kohler rule) in these optimally doped systems. To examine this relation, in figure 6(b) we plot the $\Delta\rho/\rho_{xx}(0)$ as a function of $[\mu_0 H/\rho_{xx}(0)]^2$ for NFCA with $x = 0.022$ and 0.0205 at temperatures ranging from 28 to 36 K, a temperature region which is far below the estimated Debye temperature and well above $T_{\rm c}$ within the linear-$T$ resistivity region, where the resistances due to the electron–phonon interaction, superconducting fluctuation, and flux motion can be neglected. The inset of figure 6(b) shows the corresponding data of $\Delta\rho/\rho_{xx}$ against $\tan^2\theta_{\rm H}$. As shown here, a linear-like dependence can be observed both in the $\Delta\rho/\rho_{xx}$ versus $[H/\rho_{xx}(0)]^2$ and $\Delta\rho/\rho_{xx}$ versus $\tan^2\theta_{\rm H}$ plots. As seen in figure 6(b), however, the data at different temperatures show distinctly different curves whereas the curves of $\Delta\rho/\rho_{xx}$ versus $\tan^2\theta_{\rm H}$ plots seemingly coincide, indicating that the transport properties of the nearly optimum-doping NFCA also obey the modified Kohler

rule. The violation of Kohler's rule in cuprates may be understood in terms of the non-Fermi-liquid scenario of two transport relaxation times [64], Lorentz force with MFL inelastic scattering rates [65], the anisotropic MFL model [59], or within the standard Fermi liquid theory by considering the CVC due to strong antiferromagnetic fluctuation [44]. Even though various explanations have advanced for these transverse transport anomalies in HTS cuprates or iron pnictide superconductors as we have noted, however, most theories agree that the longitudinal transport properties originate from the spin fluctuation regardless of the non-Fermi-liquid or Fermi liquid ground state taken into account in various systems [49, 50, 52, 56]. So far we can see that the new-type superconducting NFCA samples with nearly optimum doping reveal many transport properties closely resembling those of optimally doped HTS cuprates. All the characteristics of linear-$T$ resistivity, $T^2$-dependent $\cot\theta_H$, linear-$T$-like $|n_H(T)|$, and the behavior of the modified Kohler scaling rule should be simultaneously taken into account when developing theory. Recently a theory [50] has been presented to explain the unconventional Hall effect in pnictides by considering a multiband system with dominant interband interaction via spin fluctuation exchange. This theory can reproduce the main features observed experimentally, but it lacks the ability to explain magnetoresistance, which can be scaled by the modified Kohler rule, for optimum-doped HTS or iron-based superconductors. Here we do not attempt to clarify the correctness of theories and leave room for a variety of interpretations for transverse transport anomalies.

## 4. Summary

In summary, the longitudinal and Hall resistivities of superconducting NFCA single crystals with $x = 0.022$ and 0.0205 in the mixed state and in the normal state were investigated. The resistivities under magnetic fields show thermally activated behavior, and a power law magnetic field dependence of activation energy, $U \propto H^{-\alpha}$ with $\alpha =$ 0.23–0.42, has been obtained. The values of $U$, ranging from 600 K ($H = 6$ T) to 3000 K ($H = 0.25$ T), are approximately one order of magnitude smaller than those of several $10^4$ K for HTS cuprates. Due to the weak flux pinning, no sign reversal of Hall resistivities is observed in NFCA with either $x = 0.022$ or 0.0205. The correlation between mixed-state longitudinal and Hall resistivities shows the scaling behavior of $|\rho_{xy}| \propto (\rho_{xx})^{\beta}$ with the exponent $\beta \approx 2.0$, which is in agreement with theoretical predictions for weak-pinning superconductors. The anisotropic upper critical fields, coherence lengths, and the anisotropy ratio are deduced, where an anisotropy ratio $\gamma = \xi_{ab}/\xi_c = H_{c2,ab}/H_{c2,c} \approx 1.63$ is obtained for the NFCA sample with $x = 0.205$. Furthermore, the normal-state transport properties show that the anomalies of the linear-$T$ resistivity, the $T^2$-dependent cotangent of the Hall angle, the linear-$T$-like $|n_H(T)|$, and the magnetoresistance which can be scaled by the modified Kohler rule are analogous to those observed on the optimally doped HTS cuprates and other pnictides. The longitudinal resistivity can be understood within a widely accepted scenario of spin density-wave quantum critical point with strong magnetic spin fluctuation for nearly optimum-doped NFCA. The transverse resistivity requires some further explanations, in which all transport anomalies should be simultaneously taken into account.

## Acknowledgments

The authors thank the National Science Council of Taiwan for financial support under Grant No. NSC 101-2112-M-002-020-MY2 (LMW), and NSC 101-2112-M-006-010-MY3 (LJC). The single-crystal growth efforts at the University of Tennessee are supported by the US DOE, BES, through Contract No. DE-FG02-05ER46202.

## References

[1] Johnston D C 2010 *Adv. Phys.* **59** 803
[2] Stewart G R 2011 *Rev. Mod. Phys.* **83** 1589
[3] Dai P, Hu J P and Dagotto E 2012 *Nature Phys.* **8** 709
[4] Zhao K, Liu Q Q, Wang X C, Deng Z, Lv Y X, Zhu J L, Li F Y and Jin C Q 2010 *J. Phys.: Condens. Matter* **22** 222203
[5] Sun D L, Kiu Y and Kin C T 2009 *Phys. Rev.* B **80** 144515
[6] Yamamoto A *et al* 2009 *Appl. Phys. Lett.* **94** 062511
[7] Lei H, Hu R, Choi E S and Petrovic C 2010 *Phys. Rev.* B **82** 134525
[8] Lei H, Hu R and Petrovic C 2011 *Phys. Rev.* B **84** 014520
[9] Naira S, Wirtha S, Friedemanna S, Steglicha F, Sic Q and Schofield A J 2012 *Adv. Phys.* **61** 583
[10] Tanatar M A, Spyrison N, Cho K, Blomberg E C, Tan G, Dai P, Zhang C and Prozorov R 2012 *Phys. Rev.* B **85** 014510
[11] Tan G *et al* 2013 *Phys. Rev.* B **87** 144512
[12] Wang A F, Luo X G, Yan Y J, Ying J J, Xiang Z J, Ye G J, Cheng P, Li Z Y, Hu W J and Chen X H 2012 *Phys. Rev.* B **85** 224521
[13] Spyrison N, Tanatar M A, Cho K, Song Y, Dai P, Zhang C and Prozorov R 2012 *Phys. Rev.* B **86** 144528
[14] Zhou S Y *et al* 2012 arXiv:1204.3440
[15] Anderson P W 1962 *Phys. Rev. Lett.* **9** 309
[16] Kim Y B, Hempstead C F and Strnad A R 1963 *Phys. Rev.* **131** 2486
[17] Yang H C, Wang L M and Horng H E 1999 *Phys. Rev.* B **59** 8956
[18] Wang L M, Sou U-C, Yang H C, Chang L J, Cheng C-M, Tsuei K-D, Su Y, Wolf Th and Adelmann P 2011 *Phys. Rev.* B **83** 134506
[19] Wang Z D, Dong J and Ting C S 1994 *Phys. Rev. Lett.* **72** 3875
[20] Ao P 1998 *J. Phys.: Condens. Matter* **10** L677
[21] Zhu B Y, Xing D Y, Wang Z D, Zhao B R and Zhao Z X 1999 *Phys. Rev.* B **60** 3080
[22] Sato H, Katase T, Kang W N, Hiramatsu H, Kamiya T and Hosono H 2013 *Phys. Rev.* B **87** 064504
[23] Budhani R C, Liou S and Cai Z X 1993 *Phys. Rev. Lett.* **71** 621
[24] Zeldov E, Amer N M, Koren G, Gupta A, Gambino R J and McElfresh M W 1989 *Phys. Rev. Lett.* **62** 3093
[25] Palstra T T M, Batlogg B, van Dover R B, Schneemeyer L F and Waszczak J V 1990 *Phys. Rev.* B **41** 6621
[26] Abulafia Y *et al* 1996 *Phys. Lett.* **77** 1596
[27] Yeshurun Y and Malozemoff A P 1988 *Phys. Rev. Lett.* **60** 2202
[28] Wang X-L *et al* 2010 *Phys. Rev.* B **82** 024525
[29] Blatter G, Feigel'man M V, Geshkenbein V B, Larkin A I and Vinokur V M 1994 *Rev. Mod. Phys.* **66** 1125
[30] Werthamer N R, Helfand E and Hohenberg P C 1966 *Phys. Rev.* **147** 295

[31] Welp U, Kwok W K, Crabtree G W, Vandervoort K G and Liu J Z 1989 *Phys. Rev. Lett.* **62** 1908
[32] Farallel D E, Williams C M, Wolf S A, Bansal N P and Kogan V G 1988 *Phys. Rev. Lett.* **61** 2805
[33] Farallel D E, Rice J P, Ginsberg D M and Liu J Z 1990 *Phys. Rev. Lett.* **64** 1573
[34] Farallel D E, Bonham S, Foster J, Chang Y C, Jiang P Z, Vandervoort K G, Lam D J and Kogan V G 1989 *Phys. Rev. Lett.* **63** 782
[35] Martinez J C, Brongersma S H, Koshelev A, Ivlev B, Kes P H, Griessen R P, de Groot D G, Tarnavski Z and Menovsky A A 1992 *Phys. Rev. Lett.* **69** 2276
[36] Gray K E, Kampwirth R T and Farrel D E 1990 *Phys. Rev.* B **41** 819
[37] Farallel D E, Beck R G, Booth M F, Bukowski C J and Ginsberg D M 1990 *Phys. Rev.* B **42** 6758
[38] Chen G F, Li Z, Dong J, Li G, Hu W Z, Zhang X D, Song X H, Zheng P, Wang N L and Luo J L 2008 *Phys. Rev.* B **78** 224512
[39] Jaroszynski J *et al* 2008 *Phys. Rev.* B **78** 174523
[40] Welp U, Xie R, Koshelev A E, Kwok W K, Cheng P, Fang L and Wen H-H 2008 *Phys. Rev.* B **78** 140510
[41] Luo J, Orlando T P, Graybeal J M, Wu X D and Muenchausen R 1992 *Phys. Rev. Lett.* **68** 690
[42] Samoilov A V 1993 *Phys. Rev. Lett.* **71** 617
[43] Kang W N, Kim H-J, Choi E-M, Kim H J, Kim K H P and Lee S-I 2002 *Phys. Rev.* B **65** 184520
[44] Dorsey A T and Fisher M P A 1992 *Phys. Rev. Lett.* **68** 694
[45] Vinokur V M, Geshkenbein V B, Feigel'man M V and Blatter G 1993 *Phys. Rev. Lett.* **71** 1242
[46] Jin K, Butch N P, Kirshenbaum K, Paglione J and Greene R L 2011 *Nature* **476** 73
[47] Varma C M, Littlewood P B, Schmitt-Rink S, Abrahams E and Ruckenstein A E 1989 *Phys. Rev. Lett.* **63** 1996
[48] Doiron-Leyraud N, Auban-Senzier P, de Cotret S R, Bourbonnais C, Jérome D, Bechgaard K and Taillefer L 2009 *Phys. Rev.* B **80** 214531
[49] Kontani H 2008 *Rep. Prog. Phys.* **71** 026501
[50] Fanfarillo L, Cappelluti E, Castellani C and Benfatto L 2012 *Phys. Rev. Lett.* **109** 096402
[51] Tanater M A, Ni N, Martin C, Gordon R T, Kim H, Kogan V G, Samolyuk G D, Bud'ko S L, Canfield P C and Prozorov R 2009 *Phys. Rev.* B **79** 094507
[52] Anderson P W 1991 *Phys. Rev. Lett.* **67** 2092
[53] Chien T R, Wang Z Z and Ong N P 1991 *Phys. Rev. Lett.* **67** 2088
[54] Xiao G, Xiong P and Cieplak M Z 1992 *Phys. Rev.* B **46** 8687
[55] Xiong P, Xiao G and Wu X D 1993 *Phys. Rev.* B **47** 5516
[56] Stojković B P and Pines D 1996 *Phys. Rev. Lett.* **76** 811
[57] Stojković B P and Pines D 1997 *Phys. Rev.* B **55** 8576
[58] Abrahams E and Varma C M 2003 *Phys. Rev.* B **68** 094502
[59] Kokalj J, Hussey N E and McKenzie R H 2012 *Phys. Rev.* B **86** 045132
[60] Luo N and Miley G H 2009 *J. Phys.: Condens. Matter* **21** 025701
[61] Harshman D R, Dow J D and Fiory A T 2011 *Phil. Mag.* **91** 818
[62] Harris M, Yan Y F, Matl P, Ong N P, Anderson P W, Kimura T and Kitazawa K 1995 *Phys. Rev. Lett.* **75** 1391
[63] Kasahara S *et al* 2010 *Phys. Rev.* B **81** 184519
[64] Coleman P, Schofield A J and Tsvelik A M 1996 *Phys. Rev. Lett.* **76** 1324
[65] Varma C M and Abrahams E 2001 *Phys. Rev. Lett.* **86** 4652